

Supplementary Information

**Investigations of the Stability of GaAs for Photoelectrochemical H₂ Evolution in
Acidic or Alkaline Aqueous Electrolytes**

Weilai Yu¹, Matthias Richter¹, Ethan Simonoff¹, Bruce S. Brunschwig^{*2} and Nathan S. Lewis^{*1,2}

¹Division of Chemistry and Chemical Engineering and ²Beckman Institute, California Institute of
Technology, Pasadena CA, 91125

Email: nslewis@caltech.edu, bsb@caltech.edu

Experimental

A. Materials

1.0 M sulfuric acid solution (H_2SO_4 , VWR Chemicals), 1.0 M potassium hydroxide aqueous solution (KOH, TitriPUR volumetric solution and Supelco), bromine (Br_2 , reagent grade, Sigma-Aldrich), and methanol (CH_3OH , VWR Analytical, ACS, 99.8 %) were used as received. Deionized water (18.2 $\text{M}\Omega\text{ cm}$) was obtained from a Barnstead Millipore system. Single-side polished, (100)-oriented, Si-doped ($N_d = 1\text{-}5 \times 10^{17}\text{ cm}^{-3}$) n-type GaAs wafers and Zn-doped ($N_d = 1\text{-}5 \times 10^{17}\text{ cm}^{-3}$) p-type GaAs wafers were obtained from AXT Inc. Nafion (proton-exchange membrane) and Fumasep (anion-exchange membrane) were purchased from the Fuel Cell Store.

B. Electrochemical Measurements

1. Purification of electrolytes by pre-electrolysis

Prior to use in CA experiments, 1.0 M $\text{H}_2\text{SO}_4(\text{aq})$ and 1.0 M $\text{KOH}(\text{aq})$ were pre-electrolyzed in a two-compartment electrochemical cell (Pyrex), with the compartments separated by either a Nafion (acid) or Fumasep (base) membrane. Carbon rod electrodes were used as the cathode and anode, respectively. Pre-electrolysis was performed >24 h under a constant potential of >3 V or at a constant current of 6 mA. Only the catholyte was collected and used for further electrochemical measurements. No H_2O_2 was found in the catholyte after the electrolysis, as determined by spectrophotometric analysis using titanium oxalate.¹

2. Back contacts to GaAs electrodes

For n-GaAs, 100 nm of metallic In was evaporated onto the back side of the wafer. The sample was then annealed under forming gas for 10 min at 400 °C. For p-GaAs, 50 nm of metallic Ni was sputtered onto the back side of the wafer at room temperature. Sputter deposition was performed in an AJA Orion sputtering system.

3. GaAs etching

Prior to electrochemical measurements, both n-type and p-type GaAs electrodes were etched in 0.04 % (by volume) $\text{Br}_2/\text{CH}_3\text{OH}$ for 30 s, then in 1.0 M $\text{KOH}(\text{aq})$ for 15 s.² Samples were then rinsed with methanol and blown dry under a stream of $\text{N}_2(\text{g})$ for > 10 s.

4. (Photo)-electrochemical measurements

Electrochemical measurements, including chronoamperometry (CA) and cyclic voltammograms (CV), were performed in a nitrogen-filled glovebox (VAC, OMNI-LAB) with an O₂ concentration of <0.3 ppm. All electrolytes were degassed using a Schlenk line to remove the dissolved oxygen prior to transfer into the glovebox.

To facilitate XPS analysis, electrochemical measurements were performed using a custom-made compression cell fabricated from PEEK. The cell had two compartments separated by an ion-exchange membrane (Nafion for H₂SO₄, Fumasep for KOH). All electrochemical data were acquired on a SP-200 BioLogic Science Instruments potentiostat, without compensation for the solution resistance. Electrochemical measurements were performed in a three-electrode set-up, with Pt or Ni foil as the counter electrode (CE), a hydrogen electrode HydroFlex (Gaskatel) as the reference electrode (RE), and GaAs as the working electrode (WE). H₂ gas was fed into the glovebox, passed through an aqueous gas bubbler, and used to continuously purge the catholyte during electrochemical experiments. The H₂(g) from the cathode chamber and O₂(g) from the anode chamber were separately vented to outside the glove box.

Prior to each experiment, the compression cell was assembled immediately after etching of GaAs samples and transferred into the glovebox. The long-term stability of GaAs was evaluated by CA in the dark or under illumination. The *J-E* behavior of p-GaAs electrodes was periodically measured by CV during CA. Typically, the CV data were measured after a pause of 15 s at the open-circuit potential (E_{oc}), starting from $E = E_{oc} - 0.035V$ and scanning first to more negative potentials, to minimize passage of anodic current through the WE. A scan rate of 50 mV s⁻¹ was used for all CVs. After each experiment, the cell was disassembled inside the glovebox and the electrode sample was thoroughly rinsed with deionized water, blown dried with nitrogen, and stored inside the glovebox until further XPS analysis.

A miniature fiber-optic adjustable-arm light equipped with a 150 W halogen bulb was used as the illumination source and was introduced from outside the glovebox via a fiber optic. The illumination intensity at the sample position within the electrochemical cell was calibrated to 1 sun (100 mW cm⁻²) using a Si photodiode (FDS100, Thorlabs). The total volume of electrolyte in the

cathode chamber was 4 mL. For the ICP-MS analysis, 0.2 mL of electrolyte was withdrawn at intervals from the catholyte with the WE still under potential control, and the catholyte was replenished with 0.2 mL of fresh electrolyte to maintain a constant total volume of electrolyte in the cell chamber.

5. Electrodeposition of Pt and CoP catalysts

Pt was electrodeposited onto p-GaAs samples using a solution of 5 mM K_4PtCl_6 and 0.5 M KCl. A current density of -0.2 mA cm^{-2} was applied under illumination in a two-electrode configuration until a fixed charge density of -2 or -20 mC cm^{-2} had passed. A carbon rod was used as the counter electrode.

Electrodeposition of CoP onto p-GaAs samples was performed based on a published procedure.³ A “leakless” miniature AgCl/Ag electrode and a carbon rod were used as the reference and counter electrodes, respectively. The electrodeposition was performed under illumination at -1.2 V vs. AgCl/Ag until a fixed charge density of -50 , -200 , or -400 mC cm^{-2} had passed.

After each deposition, the cell was thoroughly cleaned with deionized water at least 3 times before undergoing further stability tests by CA in acidic or alkaline electrolytes.

6. Sputter deposition of Pt onto p-GaAs

Sputter deposition was performed in an AJA Orion sputtering system with a typical base pressure of $5 \times 10^{-8} \text{ Torr}$. Before deposition of Pt, p-GaAs samples were freshly etched and dried using $N_2(g)$, and promptly transferred to the sputtering chamber. The deposition of Pt was performed at room temperature under an Ar flow of 20 sccm to maintain a working pressure of 5 mTorr.

C. Analytical Methods

1. Inductively coupled plasma mass spectrometry (ICP-MS) of catholytes

Inductively coupled plasma mass spectrometry (ICP-MS) data were collected using an Agilent 8800 Triple Quadrupole ICP-MS system. Calibration solutions were prepared by diluting the multi-element standard solutions for ICP with $18.2 \text{ M}\Omega \text{ cm}$ resistivity water. The total amounts of Ga or As ions that dissolved from the electrodes were calculated and normalized to the geometric electrode area to obtain the equivalent depth of material removed from the crystalline electrode. To account for

different acidic and basic solution matrixes, standards were prepared and diluted using the same solution matrix as the analytes.

2. X-ray photoelectron spectroscopy with air-free transfer

X-ray photoelectron spectroscopy (XPS) was performed using a Kratos Axis Ultra system with a base pressure of $< 1 \times 10^{-9}$ Torr equipped with a monochromatic Al K α X-ray source with a photon energy of 1486.6 eV. Photoelectrons were collected at 0° from the surface normal with a retarding pass energy of 160 eV for survey XPS scans (step size of 1.0 eV) and for high-resolution core-level scans (step size 0.025 eV).

Prior to XPS measurements, samples were mounted on a Kratos sample holder in the glove box under N₂, and then inserted into a transfer suitcase sealed by a gate valve. The transfer suitcase was attached to the load lock of the Kratos Axis Ultra system. The load lock was pumped down to 1×10^{-6} Torr and then purged with N₂ to 1 atm. After pumping the load lock to ~ 100 Torr, the gate valve to the transfer suitcase was opened and the turbo molecular pump was switched on. After achieving a pressure of $< 1 \times 10^{-6}$ Torr, the sample was transferred into the sample transfer chamber. After closing the gate valve to the transfer suitcase, the sample was pumped down to $< 1 \times 10^{-9}$ Torr before being transferred to the analysis chamber.

Due to the high surface sensitivity that results from a low photoelectron escape depth, XPS is much more surface sensitive, and provides more direct information on the surface composition of single-crystal GaAs electrodes used in this work, than X-ray diffraction (XRD).

3. Fitting of XPS spectra

All XPS peak fitting was performed using CasaXPS software version 2.3.18. All binding energies were referenced to the adventitious carbon peak at 284.8 eV. Before fitting the data, a Shirley background was calculated and subtracted from the original spectra. The As 3d and the Ga 3d spectra were fitted to a series of 70% Gaussian/30% Lorentzian Voigt-function doublets for the 3d^{5/2} and 3d^{3/2} spin-orbit components of each peak. The peaks that comprised each doublet were constrained to have an area ratio of 3:2 and mutually identical full widths at half maximum (FWHM). The single peak of GaAs in the Ga 2p spectra was fit using an asymmetric Lorentzian function. All other peaks were fit using a 70% Gaussian/30% Lorentzian Voigt-function. The surface atomic ratios

were calculated using the relative sensitive factors (RSF) in the database of the Kratos instrument and the peak areas. The Ga/As atomic ratios were calculated based on the Ga 3d and As 3d spectra.

4. Scanning-electron microscopy (SEM)

Scanning-electron microscopy (SEM) images were obtained using a Nova NanoSEM 450 (FEI) with an accelerating voltage of 5 kV, with a working distance of 5 mm and an in-lens secondary electron detector.

5. Transmission-electron microscopy (TEM)

Transmission-electron microscopy (TEM) cross-sections of the samples were prepared using a focused Ga ion beam (FIB), on a FEI Helios NanoLab G4 Dual Beam. A carbon protection layer was applied prior to exposure to the FIB. TEM images of the prepared lamella samples were obtained using a FEI Osiris at an accelerating voltage of 200 kV equipped with a Gatan 2K TEM camera and Bruker EDS.

6. Atomic-force Microscopy (AFM)

Atomic-force microscopy (AFM) images were obtained on a Bruker Dimension Icon using Bruker ScanAsyst-Air probes (silicon tip, silicon nitride cantilever, spring constant: 0.4 N m^{-1} , frequency: 50-90 kHz), operating in the ScanAsyst mode. Images were analyzed using the Nanoscope Analysis software (version 1.9).

Figures

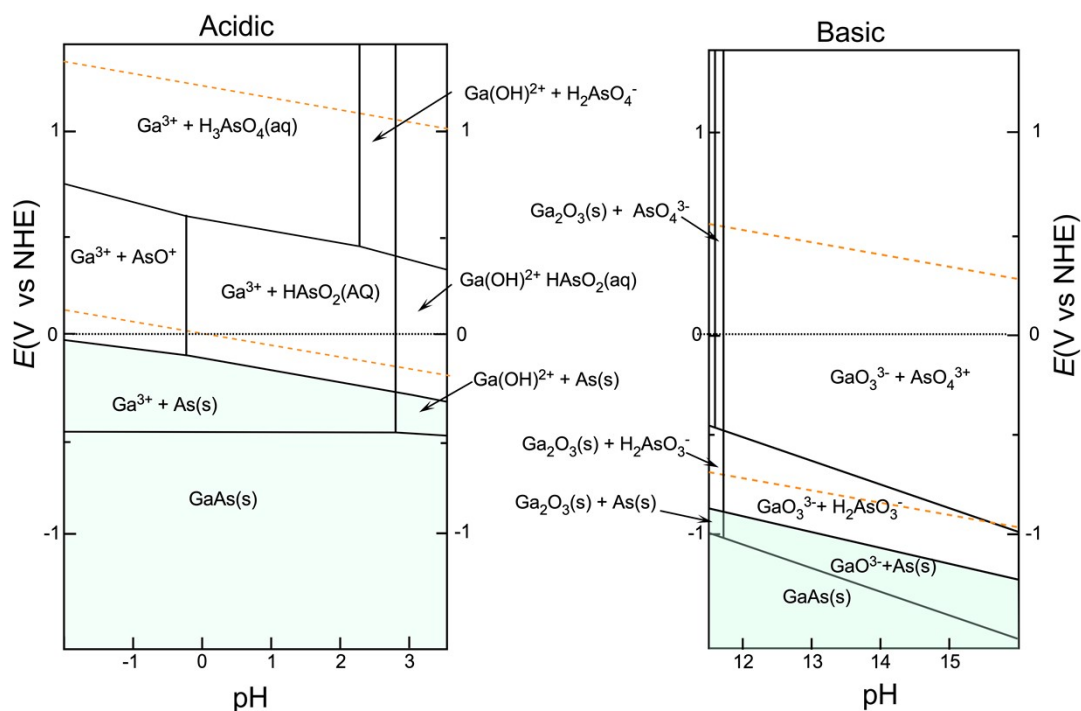


Figure S1. Calculated Pourbaix diagram of GaAs ($Ga/As = 1$) in the low (left) and high (right) pH range, as obtained from the Materials Project.⁴ The concentrations of Ga and As ions are assumed as $1 \times 10^{-8} \text{ mol kg}^{-1}$.

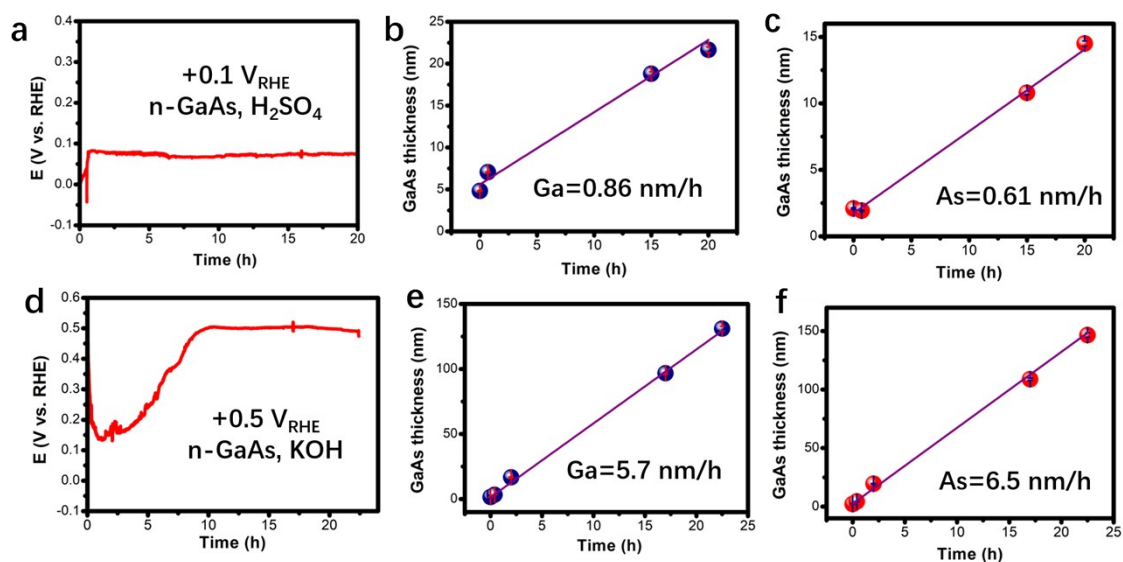


Figure S2. Corrosion rates of n-GaAs at the open-circuit potential (E_{oc}) in the dark. Comparison of (a,d) the measured E_{oc} values versus time in the dark, and the corrosion thickness of GaAs based on the concentrations of (b,e) Ga ions and (c,f) As ions in (a-c) 1.0 M $H_2SO_4(aq)$ and (d-f) 1.0 M

KOH(aq).

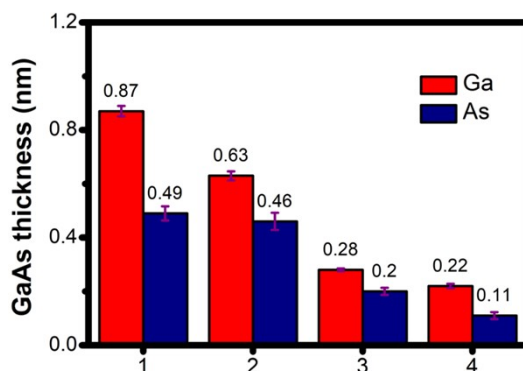


Figure S3. Comparison of initial GaAs dissolution for four different n-GaAs samples (No.1-4) when exposed to 1.0 M H₂SO₄(aq).

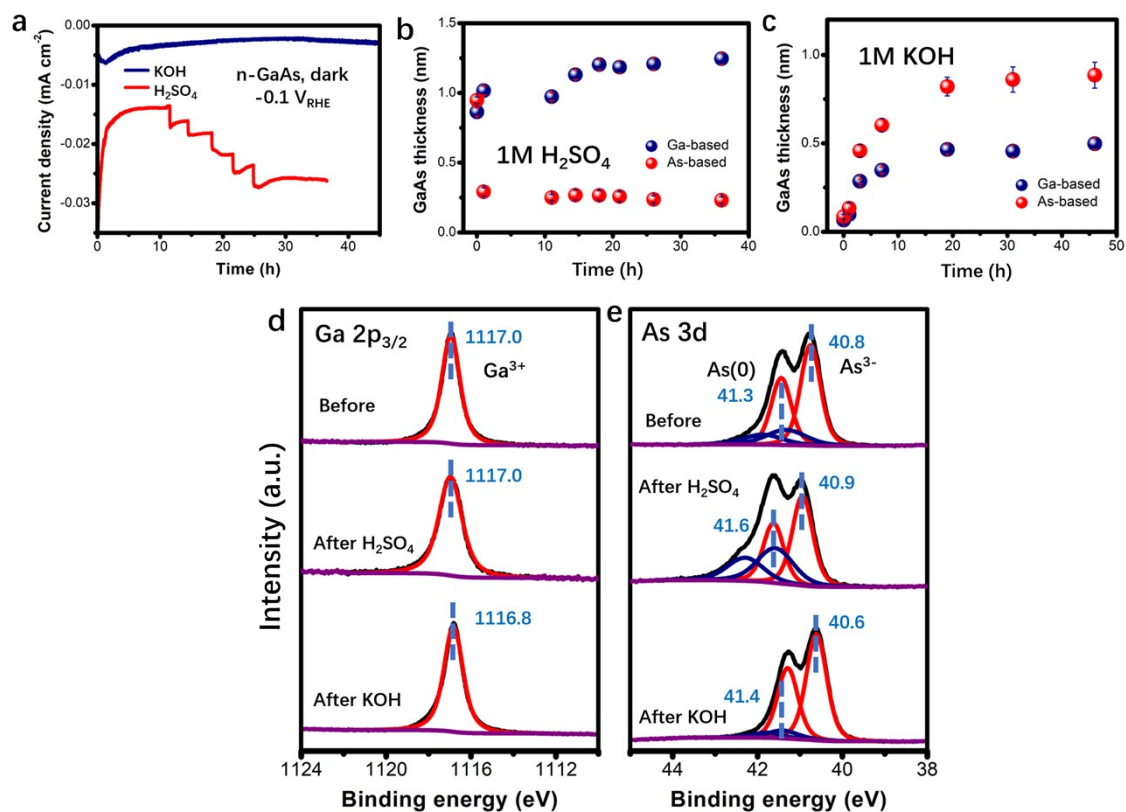


Figure S4. Results of n-GaAs electrodes evaluated at -0.1 V vs. RHE in the dark. (a) CA of n-GaAs electrodes at -0.1 V vs. RHE in the dark in 1.0 M H₂SO₄(aq) and 1.0 M KOH(aq). (b-c) Corrosion thickness (nm) of n-GaAs versus time for the electrodes evaluated in (b) 1.0 M H₂SO₄(aq) and (c) 1.0 M KOH(aq),

determined by the concentrations of dissolved Ga and As ions in the electrolyte by ICP-MS. (d-e) Comparison of XP spectra in the (d) Ga 2p_{3/2} and (e) As 3d regions for the n-GaAs electrodes before and after CA in (a).

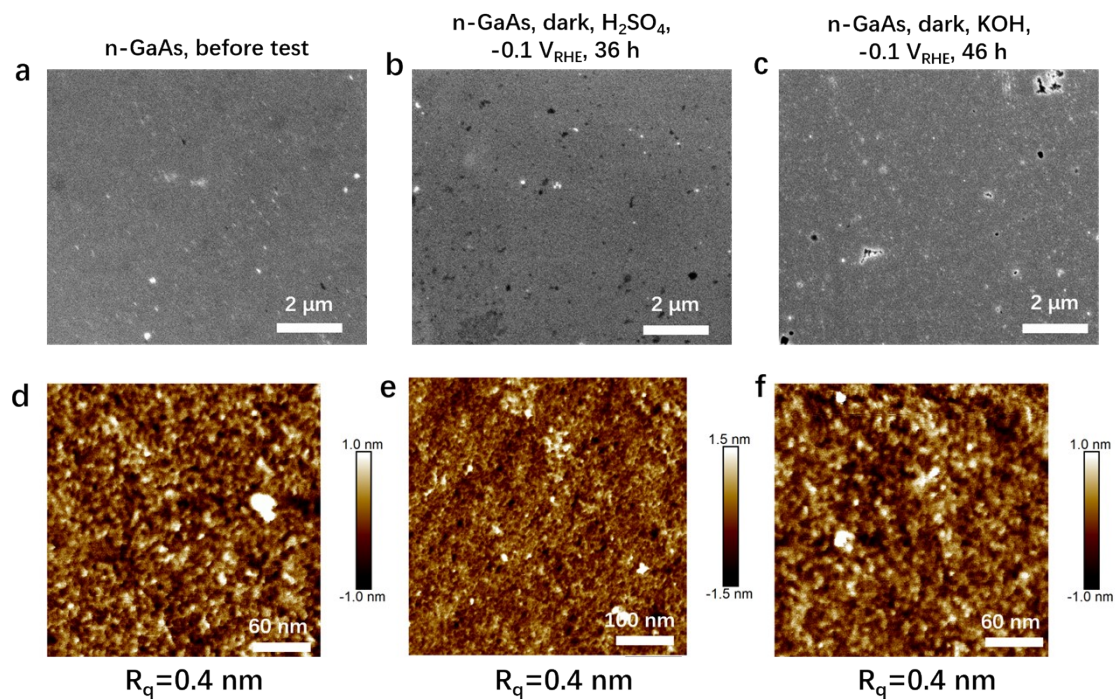


Figure S5. Comparison of SEM and AFM images of n-GaAs electrodes (a) before and, (b) after the CA at -0.1 V vs. RHE (V_{RHE}) in 1.0 M H₂SO₄(aq) in the dark for 36 h and (c) after the CA at -0.1 V vs. RHE in 1.0 M KOH(aq) in the dark for 46 h. R_q is the surface roughness.

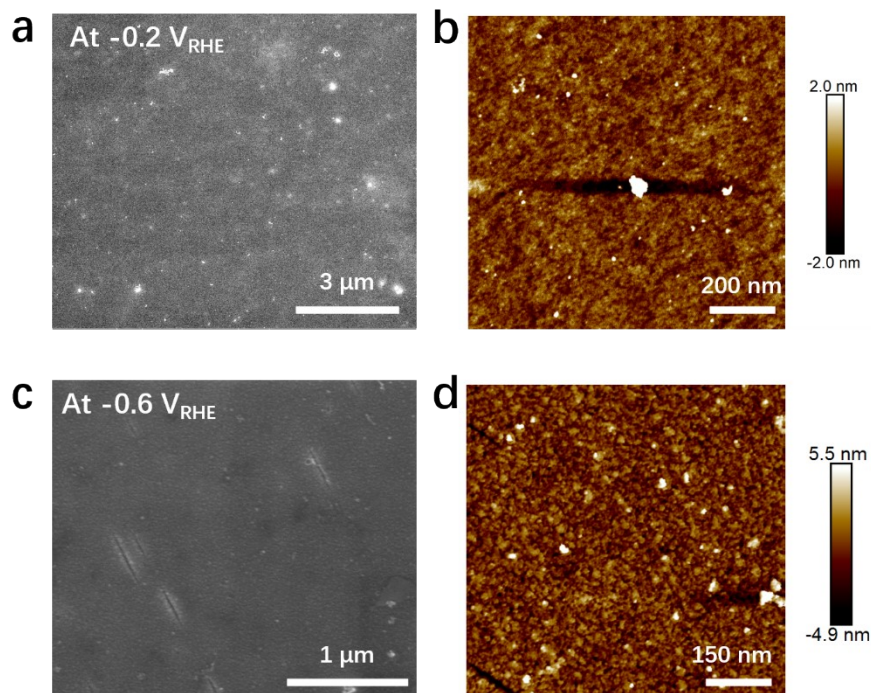


Figure S6. Comparison of (a,c) SEM and (b,d) AFM images of the etched p-GaAs electrodes after CA at (a-b) -0.2 V vs. RHE for 20 h and (c-d) -0.6 V vs. RHE for 65 h, in 1.0 M $\text{H}_2\text{SO}_4(\text{aq})$ under simulated 1-sun illumination. The surface roughness (R_q) in (b) and (d) were 0.73 and 1.3 nm, respectively.

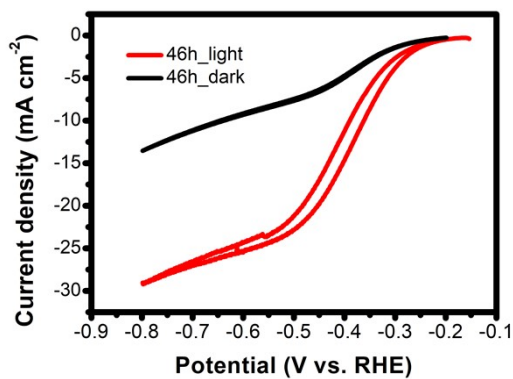


Figure S7. Comparison of the J - E behavior of an etched p-GaAs electrode in the dark (black) and under simulated 1-sun illumination (red) after 46-h of CA at $E = -0.6$ V vs. RHE in 1.0 M $\text{KOH}(\text{aq})$, showing substantial J in the dark.

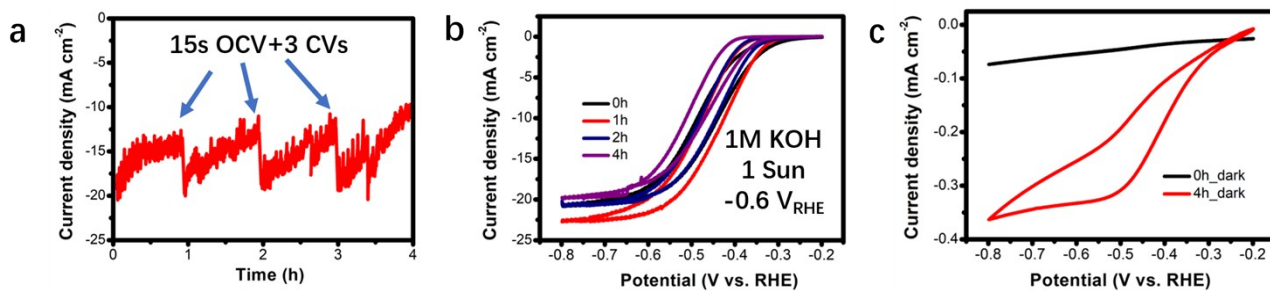


Figure S8. (a) CA of an etched p-GaAs electrode at $E = -0.6$ V vs. RHE for 4 h under simulated 1-sun illumination in 1.0 M KOH(aq). The arrows indicate hourly interruptions for collection of CV data (15 s at E_{oc} followed by three cycles of CV at 50 mV s^{-1}), (b) Comparison of the J - E behavior of a p-GaAs electrode under illumination during the CA in (a), (c) J - E behavior for a p-GaAs electrode measured in the dark in 1.0 M KOH(aq) before and after the CA in (a).

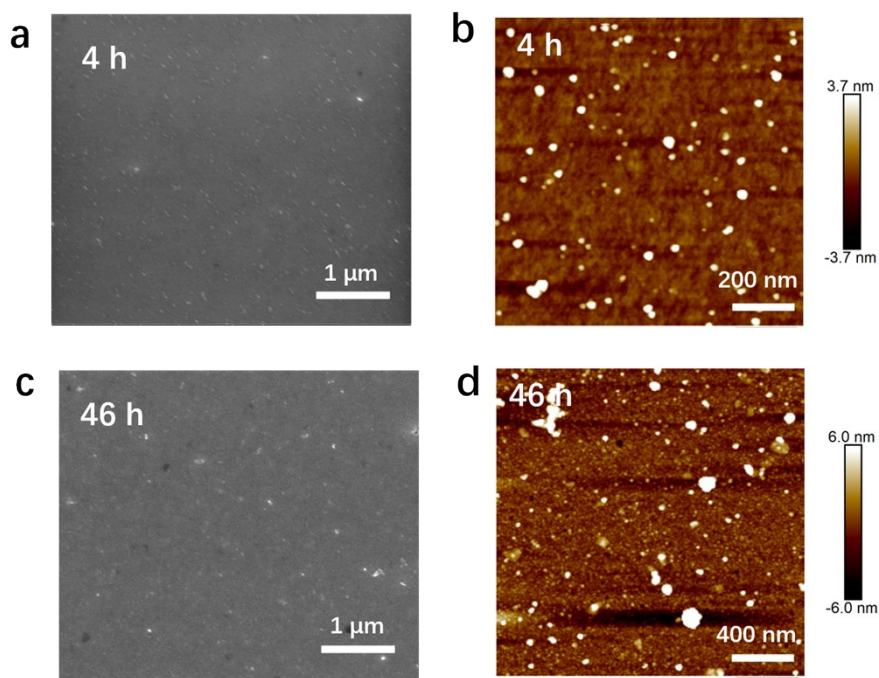


Figure S9. (a-b) SEM images and (c-d) AFM images of etched p-GaAs photoelectrodes after the CA at -0.6 V vs. RHE in 1.0 M KOH(aq) under simulated 1-sun illumination for (a,c) 4 h and (b,d) 46 h.

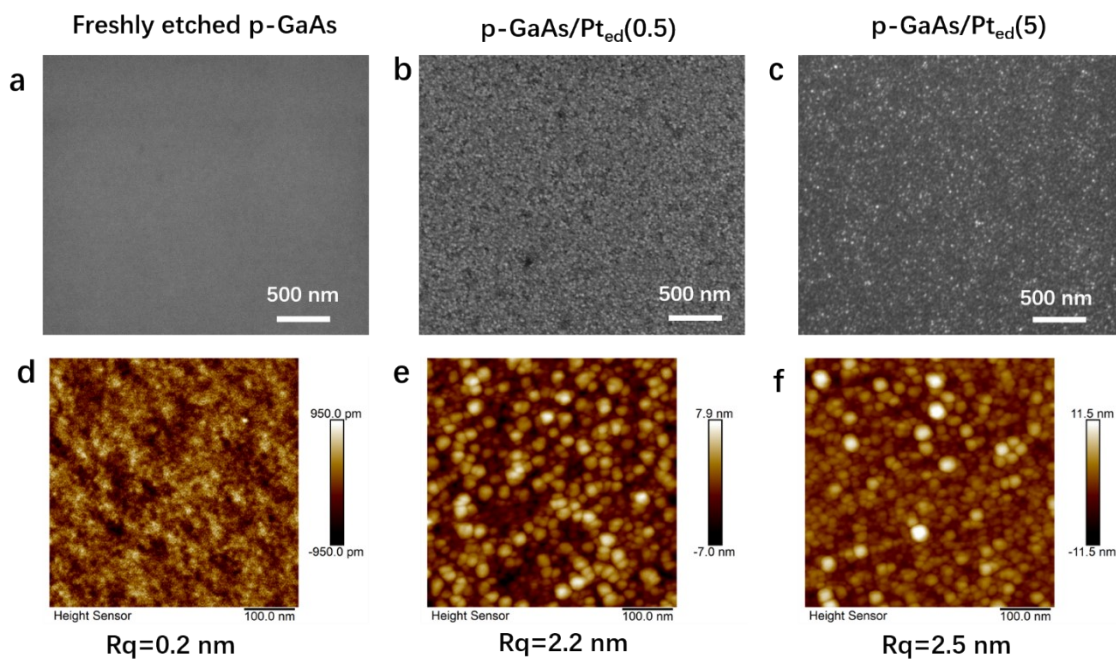


Figure S10. Comparison of (a-c) SEM and (d-f) AFM images taken for (a,d) a freshly etched p-GaAs, (b,e) an as-prepared p-GaAs/Pt_{ed}(0.5) sample and (c,f) an as-prepared p-GaAs/Pt_{ed}(5) sample. R_q is the surface roughness.

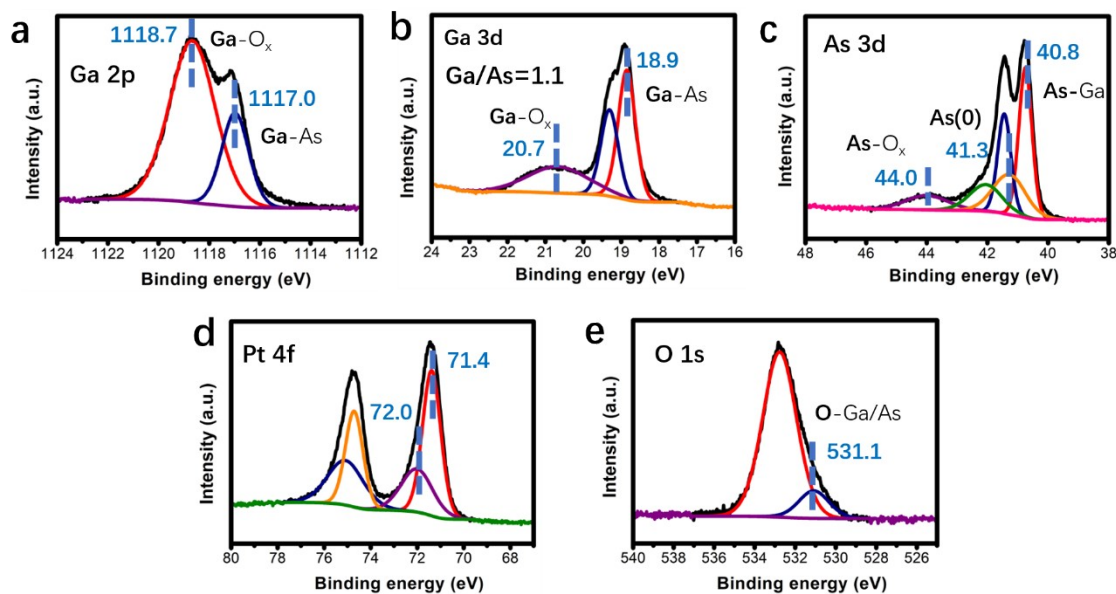


Figure S11. XP spectra in the (a) Ga 2p, (b) As 3d, (c) Ga 3d, (d) Pt 4f and (e) O 1s regions for an as-prepared p-GaAs/Pt_{ed}(0.5) electrode.

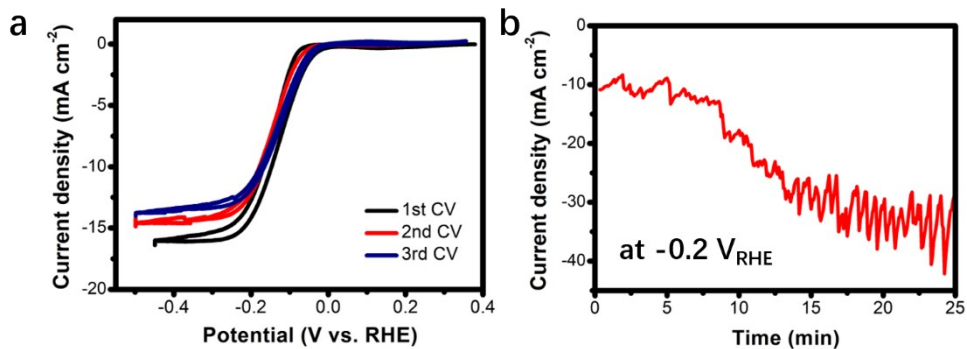


Figure S12. (a) Comparison of the first three CVs of p-GaAs/Pt_{cd}(0.5) electrode in 1.0 M H₂SO₄(aq) under simulated 1-sun illumination before the CA experiment. (b) CA of p-GaAs/Pt_{cd}(0.5) electrode in the first 25 min of CA at $E = -0.2$ V vs. RHE.

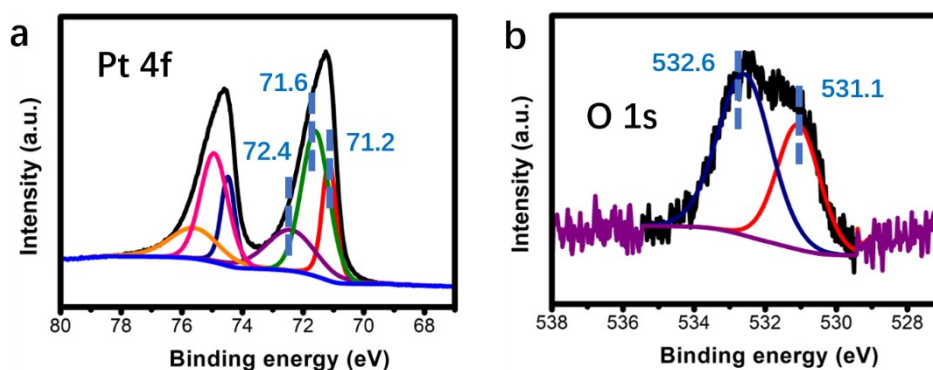


Figure S13. XPS spectra in the (a) Pt 4f and (b) O 1s regions for a p-GaAs/Pt_{cd}(0.5) electrode after CA at $E = -0.2$ V vs. RHE for 4 h in 1.0 M H₂SO₄(aq) under 1-sun illumination.

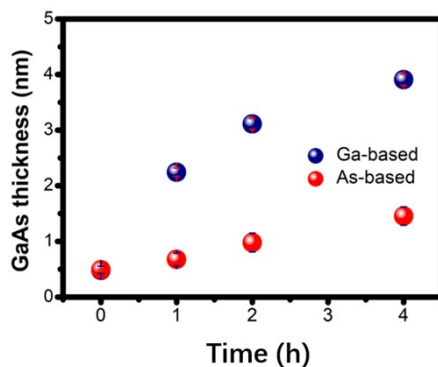


Figure S14. Corrosion thickness of GaAs vs. time for a p-GaAs/Pt_{cd}(0.5) electrode held at $E = -0.2$ V vs. RHE

in 1.0 M $\text{H}_2\text{SO}_4(\text{aq})$ under illumination.

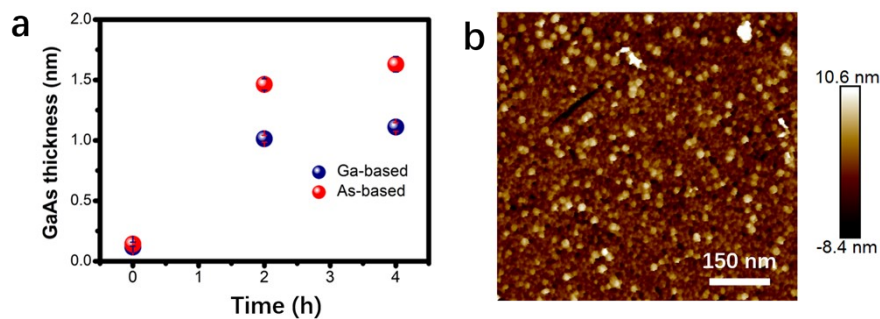


Figure S15. (a) Corrosion thickness (nm) of a p-GaAs/Pt_{ed}(0.5) electrode versus time during CA at E=-0.2 V vs. RHE in 1.0 M KOH(aq), determined by the concentrations of dissolved Ga and As ions in the electrolyte. (h) AFM image ($R_q=2.6$ nm) for the p-GaAs/Pt_{ed}(0.5) electrode after the same CA experiment in (a).

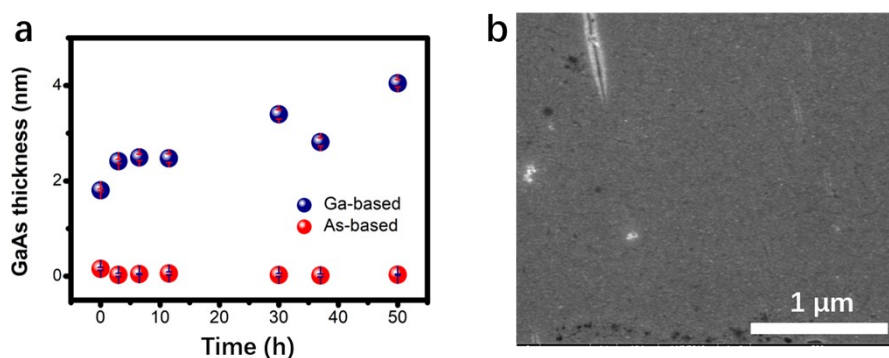


Figure S16. (a) Corrosion thickness (nm) of a p-GaAs/Pt_{ed}(5) electrode versus time during CA at E=-0.2 V vs. RHE in 1.0 M $\text{H}_2\text{SO}_4(\text{aq})$, determined by the concentrations of dissolved Ga and As ions in the electrolyte. (h) SEM image for the p-GaAs/Pt_{ed}(5) electrode after the same CA experiment in (a).

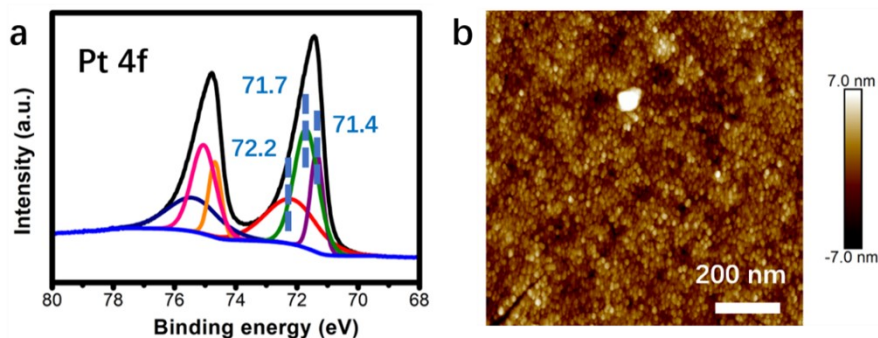


Figure S17. (a) XP spectrum in the Pt 4f region and (b) AFM image for a p-GaAs/Pt_{ed}(5) electrode after the CA at $E = -0.2$ V vs. RHE in 1.0 M H₂SO₄(aq) ($R_q \sim 1.7$ nm).

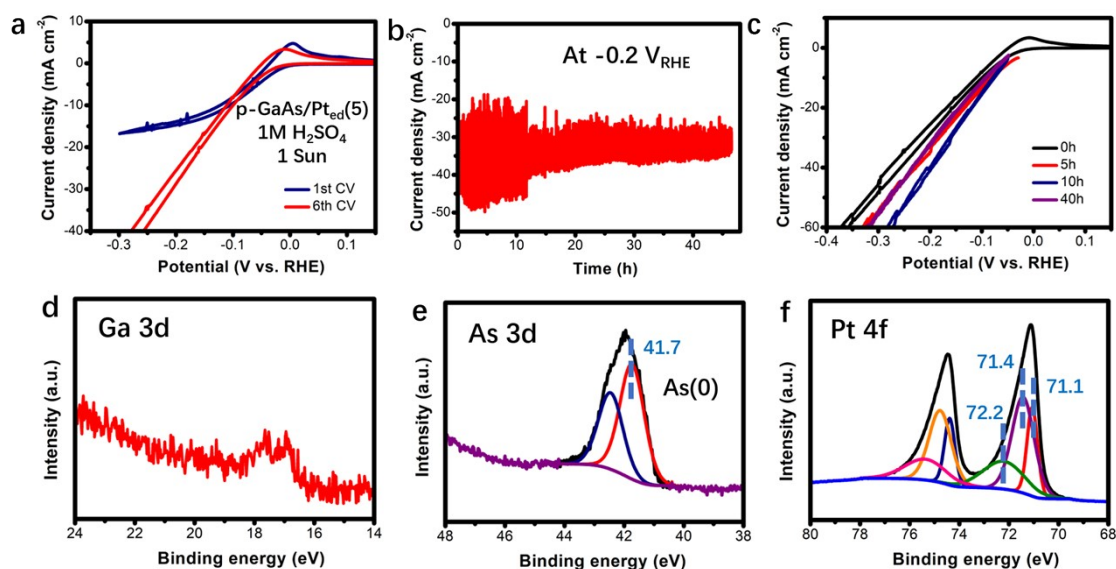


Figure S18. (a) Comparison of the 1st and the 6th J - E cycles of a p-GaAs/Pt_{ed}(5) electrode exhibiting a decrease in J_{ph} ; (b) CA of the p-GaAs/Pt_{ed}(5) electrode at $E = -0.2$ V vs. RHE under 1-sun illumination; (c-d) comparison of the J - E behavior measured periodically during CA in (b). (d-f) XPS spectra in the (d) Ga 3d, (e) As 3d and (f) Pt 4f regions for the p-GaAs/Pt_{ed}(5) electrode after CA in (b).

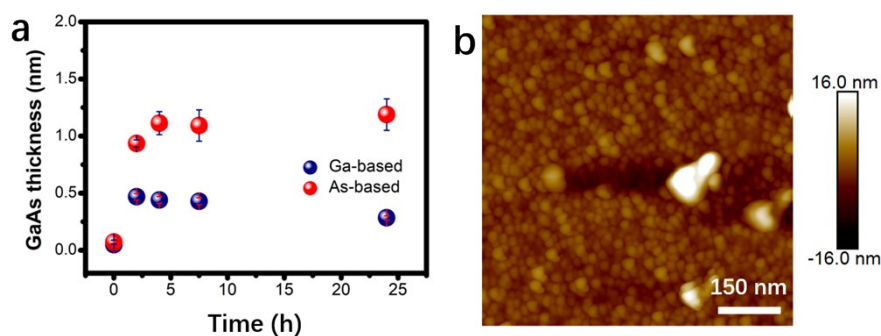


Figure S19. (a) Corrosion thickness of a p-GaAs/Pt_{cd}(5) electrode versus time during CA at $E = -0.2$ V vs. RHE in 1.0 M KOH(aq), determined by the concentrations of dissolved Ga and As ions in the electrolyte. (b) AFM image ($R_q = 2.9$ nm) for the p-GaAs/Pt_{cd}(5) electrode after the same CA experiment in (a).

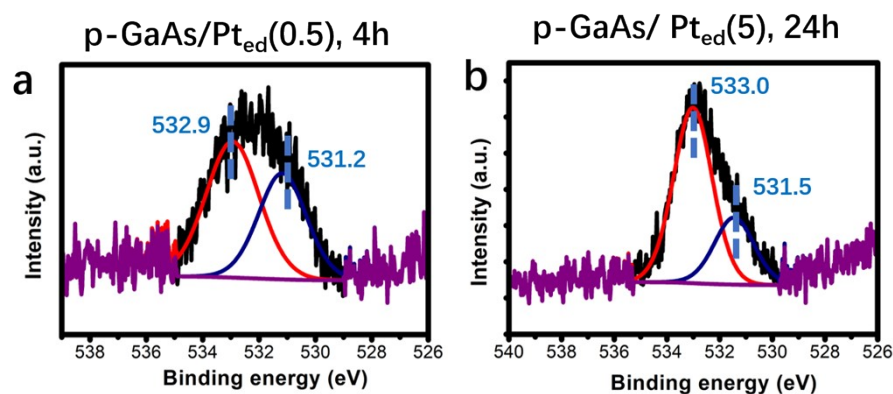


Figure S20. Comparison of XP spectra in the O 1s region for (a) a p-GaAs/Pt_{cd}(0.5) electrode after a 4-h CA and (b) p-GaAs/Pt_{cd}(5) electrode after a 24-h CA, at $E = -0.2$ V vs. RHE in 1.0 M KOH(aq) under 1-sun illumination.

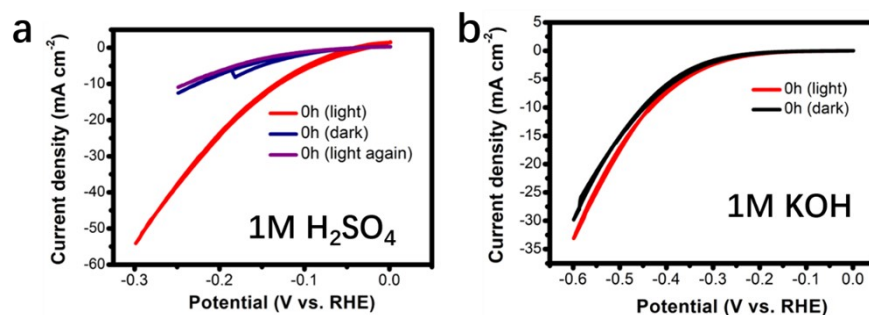


Figure S21. Comparison of the J - E behavior in (a) 1.0 M H₂SO₄ and (b) in 1.0 M KOH for p-GaAs/Pt_{sp}(5) electrodes prior to CA, under 1-sun illumination and in the dark. For (a), CVs were performed first under

illumination (red), then in the dark (blue), and again under illumination (purple).

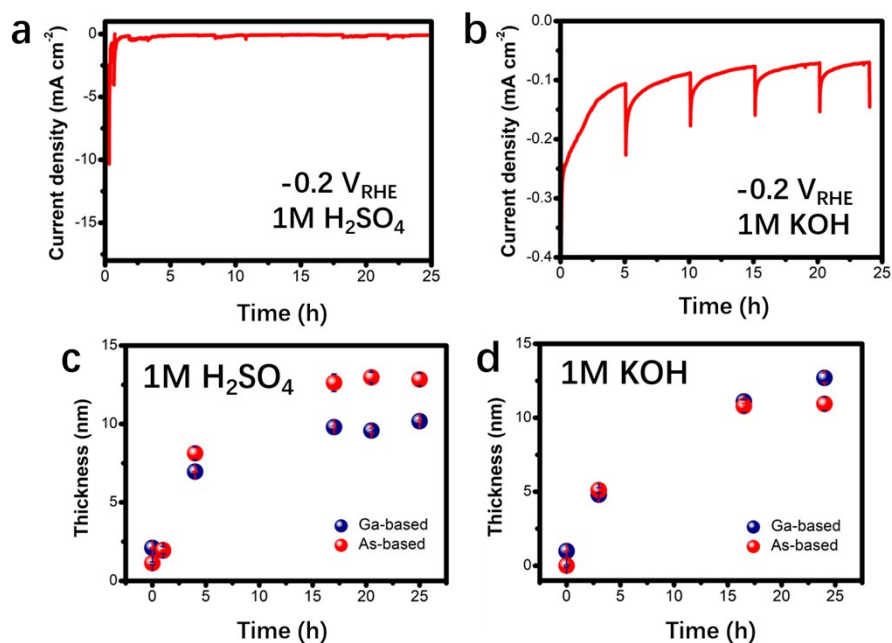


Figure S22. (a-b) CA profiles and (c-d) Corrosion thickness of GaAs vs. time for p-GaAs/Pt_{sp}(5) electrodes tested at $E = -0.2$ V vs. RHE under 1-sun illumination in (a,c) 1.0 M H₂SO₄(aq) and (b,d) 1.0 M KOH(aq).

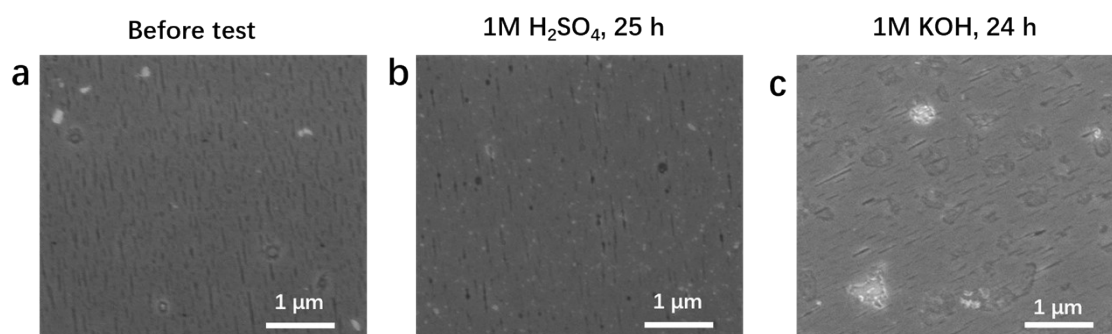


Figure S23. Comparison of SEM images of (a) an as-prepared p-GaAs/Pt_{sp}(5) sample, (b) after CA at $E = -0.2$ V vs. RHE for 25 h in 1.0 M H₂SO₄(aq) under 1-sun illumination and (c) after CA at $E = -0.2$ V vs. RHE for 24 h in 1.0 M KOH(aq) under 1-sun illumination.

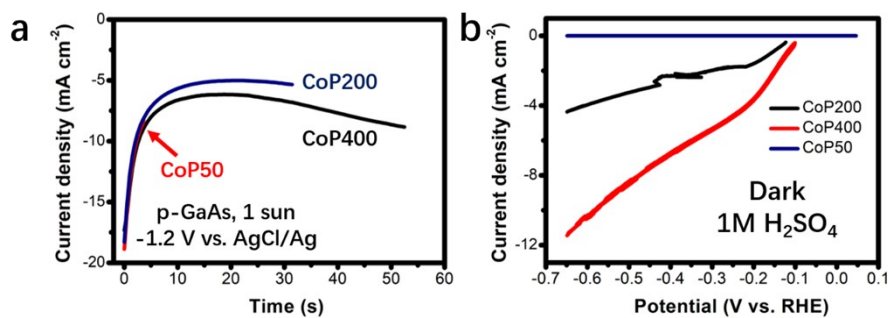


Figure S24. (a) CA of the CoP electrodeposition on p-GaAs electrode under 1-sun illumination. (b) Comparison of the J - E behaviors in the dark of as-prepared p-GaAs/CoP(x) electrodes in 1.0 M H₂SO₄(aq).

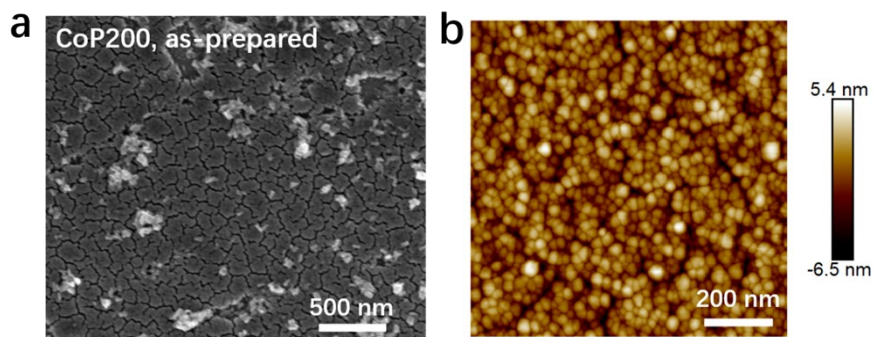


Figure S25. (a) SEM and (b) AFM images of an as-prepared p-GaAs/CoP(200) electrode.

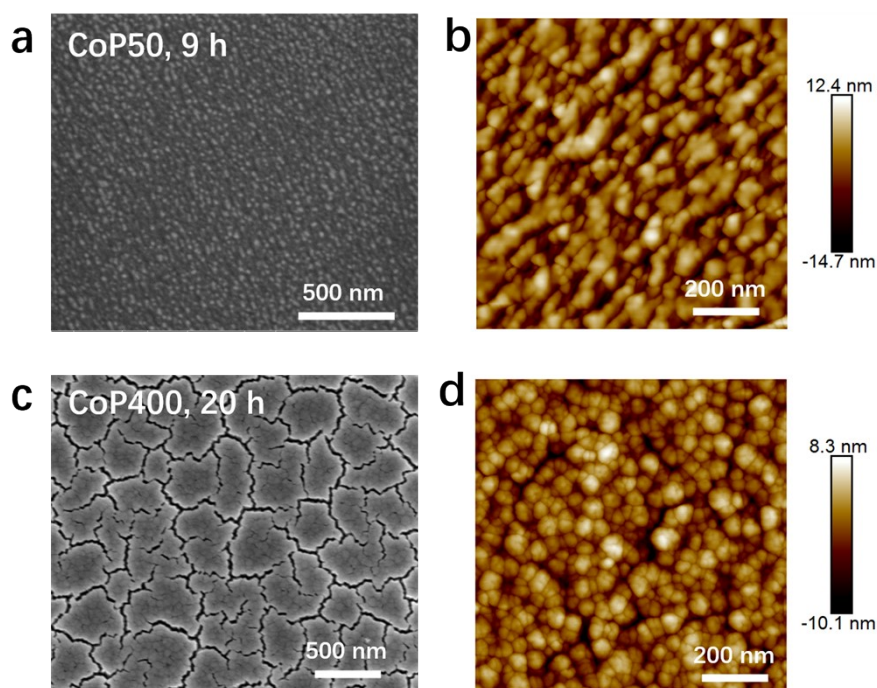


Figure S26. (a,c) SEM and (b,d) AFM images of (a-b) a p-GaAs/CoP(50) electrode after a 9-h CA at $E = -0.2$ V vs. RHE and (c-d) a p-GaAs/CoP(400) electrode after a 20-h CA at $E = -0.2$ V vs. RHE in 1.0 M $\text{H}_2\text{SO}_4(\text{aq})$ under 1-sun illumination.

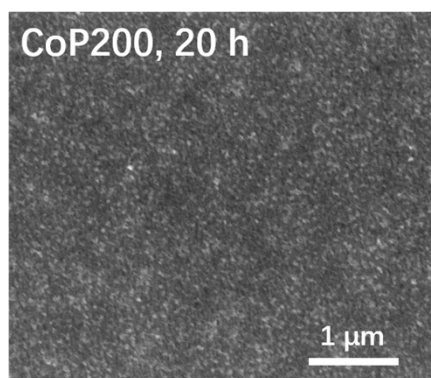


Figure S27. SEM image of (a-b) a p-GaAs/CoP(200) electrode after a 20-h CA at $E = -0.2$ V vs. RHE in 1.0 M $\text{H}_2\text{SO}_4(\text{aq})$ under 1-sun illumination.

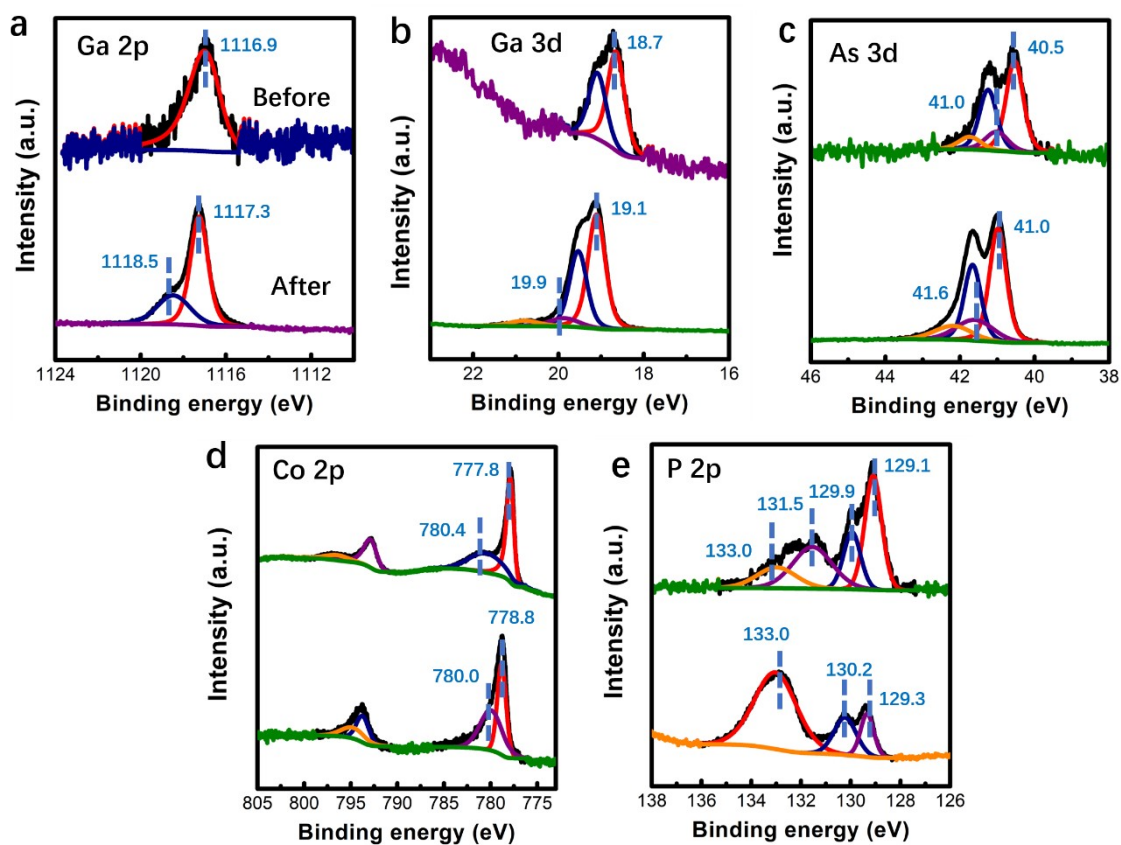


Figure S28. Comparison of XP spectra in the (a) Ga 2p, (b) Ga 3d, (c) As 3d, (d) Co 2p and (e) P 2p regions

for a p-GaAs/CoP(200) electrode before and after the 20-h CA at $E = -0.2$ V vs. RHE in 1.0 M H₂SO₄(aq) under 1-sun illumination.

References

- 1 K. Liu, J. C.-C. Yu, H. Dong, J. C. S. Wu and M. R. Hoffmann, *Environmental Science & Technology*, 2018, **52**, 12667–12674.
- 2 S. Hu, M. R. Shaner, J. A. Beardslee, M. Lichterman, B. S. Brunschwig and N. S. Lewis, *Science*, 2014, **344**, 1005.
- 3 F. H. Saadi, A. I. Carim, E. Verlage, J. C. Hemminger, N. S. Lewis and M. P. Soriaga, *The Journal of Physical Chemistry C*, 2014, **118**, 29294–29300.
- 4 K. A. Persson, B. Waldwick, P. Lazic and G. Ceder, *Physical Review B*, , DOI:10.1103/PhysRevB.85.235438.

Table S1. Corrosion rates of GaAs electrodes determined by ICPMS in 1.0 M H₂SO₄ and KOH.

Electrode	Electrolyte	CA	V _{app}	Ga etch Rate ²	As Etch Rate ²
	1.0 M	h	V _{RHE}	nm h ⁻¹ x 10 ²	nm h ⁻¹ x 10 ²
n-GaAs	H ₂ SO ₄	20	OC ¹	85	60
n-GaAs	H ₂ SO ₄	36	-0.1	1	0
n-GaAs	KOH	22.5	OC ¹	573	640
n-GaAs ³	KOH	46	-0.1	1	0
p-GaAs	H ₂ SO ₄	72	OC ¹	17	15
p-GaAs	H ₂ SO ₄	20	-0.2	13	0
p-GaAs	H ₂ SO ₄	65	-0.6	9	0
p-GaAs	KOH	26	OC ¹	658	669
p-GaAs ³	KOH	46	-0.6	0	2
p-GaAs/Pt _{cd} (5)	H ₂ SO ₄	50	-0.2	4	0
p-GaAs/Pt _{cd} (5) ³	KOH	24	-0.2	1	4
p-GaAs/P _{tsp} (5) ³	H ₂ SO ₄	25	-0.2	30	43
p-GaAs/Pt _{sp} (5) ³	KOH	24	-0.2	49	45
p-GaAs/Pt _{cd} (0.5)	H ₂ SO ₄	4	-0.2	88	24
p-GaAs/Pt _{cd} (0.5)	KOH	4	-0.2	25	38

¹ Open Circuit; ²Average rates were calculated by dividing the total loss of Ga/As ions by the whole duration of CA; ³Total dissolution of Ga/As plateaued over time

Table S2. Summary of XPS results for GaAs electrodes.

Electrode	Electrolyte	E	Time	Ga	As	Ga	Ga/As	As ⁰ /As	As ³⁺ /As	Ga ³⁺ /Ga	Ga ³⁺ /As ³⁺	As ⁰ /As ³⁺
		V _{RHE}	h	2p _{3/2}	3d _{3/2}	3d _{3/2}	3d					
				eV	eV	eV						
n-GaAs	none			1117	40.8, 41.3	–	0.24	0.22±0.01	0.78			0.28
n-GaAs	H ₂ SO ₄	-0.1	36	1117	40.9, 41.6	–	0.2	0.41±0.01	0.59			0.69
n-GaAs	KOH	-0.1	46	1116.8	40.6, 41.4	–	0.34	0.11±0.02	0.89			0.12
p-GaAs	none			1116.9	40.6, 41.1	18.8	0.94	0.22±0.05	0.78	1	1.21	0.28
p-GaAs	H ₂ SO ₄	-0.2	20	1117.1	40.8, 41.5	18.9	1.1	0.13±0.04	0.87	1	1.26	0.15
p-GaAs	H ₂ SO ₄	-0.6	65	1117.2	40.9, 41.5	19	0.98	0.28±0.03	0.72	1	1.36	0.39
p-GaAs	KOH	-0.6	4	1117.2	40.8, 41.3	18.9	1.4	0.17±0.03	0.72	1	1.94	0.39
p-GaAs	KOH	-0.6	46	1117	40.5, 41.3	18.7	1.1	0.13±0.05	0.87	1	1.26	0.15
p-GaAs/Pt _{cd} (0.5)	none			1117.0, 1118.7	40.8, 41.3, 44.0	18.9, 20.7	1.1	0.36±0.06	0.54	0.7	1.43	0.67
p-GaAs/Pt _{cd} (0.5)	H ₂ SO ₄	-0.2	4	–	41.3, 41.8, 42.7	19.0	0	0.53±0.13	0.16	0	0	3.31
p-GaAs/Pt _{cd} (5)	H ₂ SO ₄	-0.2	50	–	42.1	–	0	1	0	0	0	
p-GaAs/Pt _{cd} (0.5)	KOH	-0.2	24	1117.1, 1117.9	41.0, 41.7, 42.9	19.1, 20.0	1.3	0.67±0.11	0.47	0.75	2.07	1.43
p-GaAs/Pt _{cd} (5)	KOH	-0.2	4	1116.6, 1117.1	40.7, 41.6	18.5, 19.0	0.71	0.44±0.03	0.56	0.81	1.03	0.79
p-GaAs/Pt _{sp}	none			1116.7, 1118.4	40.6, 41.4	18.6	1.2	0.58±0.3	0.42	1	2.86	1.38
p-GaAs/Pt _{sp}	H ₂ SO ₄	-0.2	25	–	41.6	19	0.11	0.76±0.06	0	1		
p-GaAs/Pt _{sp}	KOH	-0.2	24	1116.8, 1118.0	41.1, 41.9, 43.8	19	0.39	0.33±0.06	0.32	1	1.22	1.03
p-GaAs/CoP200	none			1116.9	40.5, 41.0	18.7	0.72	0.22±0.15	0.78	1	0.92	0.28
p-GaAs/CoP50	H ₂ SO ₄	-0.2	9	1117.1	40.8, 41.5	19	1	0.16±0.02	0.84	1	1.19	0.19
p-GaAs/CoP200	H ₂ SO ₄	-0.2	20	1117.3, 1118.5	41.0, 41.6	19.1, 19.9	0.9	0.28±0.02	0.72	0.89	1.11	0.39
p-GaAs/CoP400	H ₂ SO ₄	-0.2	20	–	40.6, 41.4, 43.3	18.7	0.14	0.20±0.05	0.45	1	0.31	0.44